Non-Invasive Atrial Fibrillation Driver Localization Using Recurrent Neural Networks and Body Surface Potentials

Miriam Gutiérrez-Fernández-Calvillo[a], Miguel Ángel Cámara-Vázquez[a], Ismael Hernández-Romero[b], María S Guillem[b], Andreu M Climent[b], Óscar Barquero-Pérez[a]

[a] Universidad Rey Juan Carlos, Fuenlabrada, Madrid, Spain
[b] ITACA Institute, Universitat Politècnica de València, València, Spain

Abstract

Ablation is the main therapy to control Atrial Fibrillation (AF). However, the underlying mechanism for AF initiation and maintenance remains mostly unknown and represent a major challenge. ECG Imaging (ECGI) has been presented to address this issue, but it is an ill-posed problem and presents several limitations. Many Deep Learning methods have been proposed for AF characterization, but few provide a solution involving the location of the AF driver. In this work, we propose finding the location of AF drivers using Body Surface Potentials (BSPs) and CNN-LSTM with an attention layer networks as a supervised classification problem. The AF driver was correctly located the 94.42% of the time with an average Cohen's Kappa of 0.87. Hence, the proposed model could provide an effective solution for identifying AF driver location for ablation procedures as a non-invasive approach.

1. Introduction

Atrial Fibrillation (AF) is the most common sustained cardiac rhythm disorder, and it is linked to increased morbidity from thromboembolism, heart failure, ischemic stroke, and a lower quality of life [1]. The prevalence of AF is rising sharply in developed countries, indicating a major health issue [2]. The most effective method to restore sinus rhythm, and consequently relieve the symptoms, involves catheter-based ablation through surgery [3].

It is known that there are multiple electric mechanisms reported to initiate and maintain AF activity, such as atrial wavelets, macroreentries and localized sources [4]. Therefore, in order to effectively ablate these areas that sustain the arrhythmia, it is essential to locate and characterize them. AF drivers location can be accomplished through invasive electrophysiological (EP) studies or non-invasive methods [5]. With this aim, ECG Imaging (ECGI) techniques have been proposed to locate AF drivers, although this approach presents some limitations [6–8].

Machine Learning (ML) and Deep Learning (DL) have disrupted healthcare by enabling more powerful and effective diagnosis and treatment techniques, such as AF characterization and detection. Previous research has shown the ability and potential DL yields for AF characterization and detection [9–11].

We propose a hybrid form of CNN-LSTM with an attention layer, which enables feature extraction and sequential data modeling, to find the region of the atria where the AF driver is allocated using BSP signals [12, 13]. As a result, we address the problem as a supervised classification task using labeled realistic computerized AF and torso models.

2. Methods

2.1. Computerized Models

EGMs and BSPs were obtained employing one realistic computerized model of atria geometry (N=2039 nodes) and 10 models of torso geometry (M=659) [8, 12, 14], considering a simplified endocardium-epicardium layer for the atrial tissue [15]. A total of 13 AF models were generated from multiple complexity propagation patterns and driver locations. Given the experimental conditions, the AF driver can be allocated in the following anatomical regions: right atria (RA), left atria (LA) or no driver detection. The resulting signals, which ranged from 2 to 5 s, were sampled at $fs = 500Hz$.

2.2. AF Driver Location as a classification Problem

We propose to address the characterization of AF by locating its drivers as a supervised multi-class classification problem. Hence, we divided the atria geometry into 2 regions: Right Atria (RA) assigned as class 1, Left Atria (LA) assigned as class 2 and assigning class 0 when no driver is found. Each time instant of the BSP was assigned one class from 0-2 following a manual labeling approach.

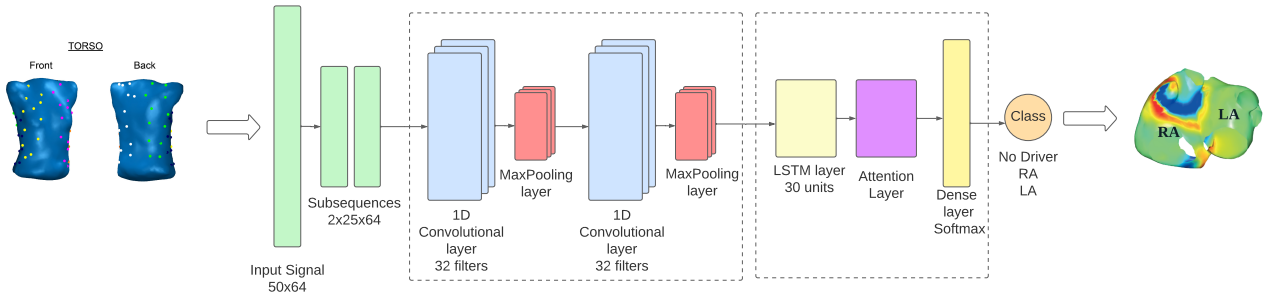

Figure 1. CNN-LSTM architecture schematic overview

BSP signals were computed solving the forward problem of electrocardiography using each of the 10 torso models and 13 AF models. Following, signals were referenced to the Wilson Central Terminal (WCT), corrupted with Gaussian noise to 20 dB and filtered them using a 4^{th}-order bandpass Butterworth filter (fc_1=3 Hz and fc_2=30Hz) [8, 12]. Hence, 130 BSP models were obtained, from which only 64 nodes were selected in order to simulate a realistic multi-electrode vest used in electrophysiological studies.

2.3. Long-Short Term Memory Networks (LSTM) Architectures and Attention Mechanisms

RNN are a family of neural networks (NN) for sequence data processing and modeling very popular among natural language processing and signal applications. Unlike conventional NN, RNN enables an appropriate generalization across the different samples of the signal [16]. LSTM networks are a type of RNN that overcomes the major issues conventional RNN encounters: difficulty to process very long sequences. In contrast, LSTM networks include mechanisms to selectively forget or update the information that is propagated across the network [17].

In many tasks, attention mechanisms have become an essential component of sequence modeling and transduction models, allowing modeling of dependencies regardless of their distance in the input or output sequences. These attention techniques are often used in combination with RNN or LSTM to maximize its performance [18].

2.4. Convolutional Neural Network (CNN) Architectures

Commonly employed in computer vision, CNNs use convolutional and pooling layers to extract spatial features from input data. Various filters or kernels are convolved to the input array in convolutional layers generating various feature maps. The subsequent layer, the pooling layer, reduces the spatial scale of the convolutional layer output. Since these layers are frequently followed by a dense layer, the output of the convolutional network must first be flattened [19].

2.5. CNN-LSTM Architectures

CNN-LSTM models are hybrid architectures that combine LSTM layers for time series classification with CNN layers for feature extraction from input sequences. In order to accomplish this task, the original sequence is divided into smaller blocks that are fed to convolutional networks, which will extract features from each of the subsequences. The retrieved features from each block will then be interpreted by LSTM layers, enabling the sequence classification.

We propose an architecture based on two main modules: CNN and LSTM. The CNN module is comprised of two subsequential 1D Time distributed convolutional layers of 32 filters followed by two max-pooling layers of size (5×5) and (3×3). Then, the output of this module is passed through a 30-unit LSTM layer and a self-attention layer of size 10. Finally, the output is passed through a 3-unit dense layer with a softmax activation function in order to perform the classification. Furthermore, dropout layers are added to avoid overfitting in the results.

2.6. Performance Metrics

Different metrics were utilized to measure the goodness of the models globally (Accuracy) and by regions (Recall and Precision)

- Accuracy (Acc). Used as a global metric, it yields the proportion of correctly predicted driver regions to the total observations:

$$Acc = \frac{TP + TN}{Total} \tag{1}$$

- Cohen's Kappa (κ). It is a robust statistic that aims to rate reliability of results, computed as:

$$\kappa = \frac{p_0 - p_e}{1 - p_e} \tag{2}$$

where p_0 is the relative agreement among raters (identical to accuracy), and p_e is the the hypothetical probability of chance agreement. As a result, a score of 1 denotes complete agreement amongst raters, whereas a score of 0 denotes the level of agreement that would be predicted by chance alone.

• Recall (or True positive rate, TPR). It represents the percentage of positive drivers for a given region that are correctly classified:

$$Recall = \frac{TP}{TP + FN} \tag{3}$$

• Precision. It provides an insight on of all drivers classified in a region, how many are actually located in that region:

$$Precision = \frac{TP}{TP + FP} \tag{4}$$

where TP (true positives), FP (false positive), TN (true negatives) and FN (false negatives).

2.7. Experimental set-up

The final feature dataset consists of 120 AF models and one sinus rhythm model arranged sequentially into a matrix with size (29,000 time instants $\times$ 64 nodes). Additionally, for every time instant of the signals, one class (1 or 2 for the corresponding atria region or 0 if there is no driver) is included in the labels' array. Morever, BSPs were downsampled to $fs = 50Hz$ to avoid feeding the network with redundant batches, since AF spectral activity is bounded between 2.5 and 25 Hz [20].

A 4-fold cross validation scheme was developed to validate the results aiming to accomplish statistic significance. Each BSP signal was divided into train and test batches of 50 samples each, to preserve temporal correlation. The mean and standard deviation of the 4-folds are used to calculate the final performance of the models.

3. Results

The obtained results show an average accuracy of 0.944 ± 0.043 and a mean Cohen's Kappa of 0.87 in the test set, indicating a very satisfactory overall performance and little variation between folds. The confusion matrix depicted in Figure 2 shows the average and standard deviation of the normalized count of true and predicted instances in the 4-folds. Although the 3 regions provide excellent performance, the results are better when detecting LA drivers.

Attending to the results by region depicted in Figure 3, the class which presents the highest positive predictive value with the slightest deviation among folds is LA, although the three classes show very high values. It is important to take into account the high cost associated to do not

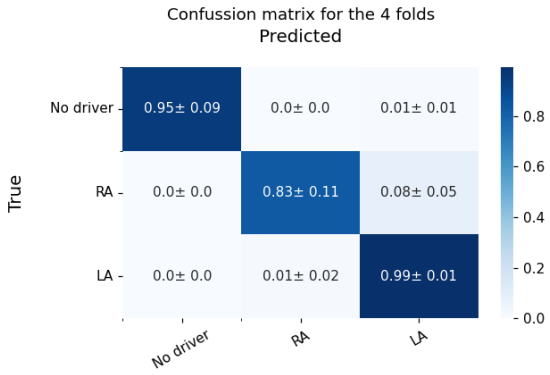

Figure 2. Confusion matrix obtained for the test set and the 4-folds

detecting the driver's location correctly, which in practice may result in an inappropriate ablation of the endocardium and the persistence of the arrhythmia. On the opposite, analyzing the precision, the class which presents the largest variance among folds is LA, which may be due to imbalance in the dataset.

4. Discussion and conclusions

The proposed CNN-Attention LSTM methodology could outperform the current solutions for AF driver detection based on ECGI. This method has provided very promising results for three regions of the atria and 20 dB noise level.

However, this model entails some limitations that must be overcome. The major drawback is the scarce data: only 13 AF models, 10 torso geometries, and one atrial geometry are used in this study. Hence, the 130 resulting BSPs sets may not be enough to provide an adequate generalization, since some underlying leakage may occur. Therefore, it is essential to incorporate more models and geometries which may enable the configuration of some other validation schemes: cross-validation by AF model or by ge-

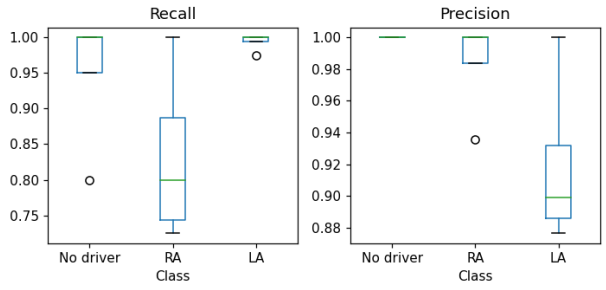

Figure 3. Average and standard deviation of the recall and precision obtained for each class

ometries. Additionally, more data would signify a more balanced and stratified dataset in terms of the labels.

Regarding some future work research lines, we consider increasing significantly the number of regions to provide a more accurate and precise location of the driver. Furthermore, real patient data could be employed to validate the results, although tagging the real models may be challenging from a clinical and technical point of view. Moreover, the project scope aims to characterize AF driver location, for which EGM regression based on BSPs will be investigated through more complex Deep Learning approaches.

Acknowledgements

This work has been partially supported by: Ministerio de Ciencia e Innovación (PID2019-105032GB-I00), Instituto de Salud Carlos III, and Ministerio de Ciencia, Innovación y Universidades (supported by FEDER Fondo Europeo de Desarrollo Regional PI17/01106 and RYC2018-024346B-750), Consejería de Ciencia, Universidades e Innovación of the Comunidad de Madrid through the program RIS3 (S-2020/L2-622), EIT Health (Activity code 19600, EIT Health is supported by EIT, a body of the European Union) and the European Union's Horizon 2020 research and innovation program under the Marie Skłodowska-Curie grant agreement No. 860974.

References

[1] Lip GY, Tse HF. Management of atrial fibrillation. The Lancet 2007;370(9587):604–618.

[2] Chugh SS, Havmoeller R, Narayanan K, Singh D, Rienstra M, Benjamin EJ, Gillum RF, Kim YH, McAnulty Jr JH, Zheng ZJ, et al. Worldwide epidemiology of atrial fibrillation: a global burden of disease 2010 study. Circulation 2014;129(8):837–847.

[3] Pritchett EL. Management of atrial fibrillation. New England Journal of Medicine 1992;326(19):1264–1271.

[4] Guillem M, Climent A, Rodrigo M, Fernández-Avilés F, Atienza F, Berenfeld O. Presence and stability of rotors in atrial fibrillation: evidence and therapeutic implications. Cardiovascular Res 2016;109(4):480–492.

[5] Haissaguerre M, Hocini M, Denis A, Shah AJ, Komatsu Y, Yamashita S, Daly M, Amraoui S, Zellerhoff S, Picat MQ, et al. Driver domains in persistent atrial fibrillation. Circulation 2014;130(7):530–538.

[6] Haissaguerre M, Hocini M, Shah AJ, Derval N, Sacher F, Jais P, Dubois R. Noninvasive panoramic mapping of human atrial fibrillation mechanisms: A feasibility report. Journal of Cardiovascular Electrophysiology 2013; 24(6):711–717.

[7] Rodrigo M, Climent AM, Liberos A, Calvo D, Fernández-Avilés F, Berenfeld O, et al. Identification of dominant excitation patterns and sources of atrial fibrillation by causality analysis. Annals of Biomedical Engineering 2016; 44(8):2364–2376.

[8] Pedrón-Torrecilla J, Rodrigo M, Climent A, Liberos A, Pérez-David E, Bermejo J, et al. Noninvasive estimation of epicardial dominant high-frequency regions during atrial fibrillation. J Cardiovascular Electrophysiol 2016; 27(4):435–442.

[9] Xia Y, Wulan N, Wang K, Zhang H. Detecting atrial fibrillation by deep convolutional neural networks. Computers in biology and medicine 2018;93:84–92.

[10] Mousavi S, Afghah F, Acharya UR. Han-ecg: An interpretable atrial fibrillation detection model using hierarchical attention networks. Computers in biology and medicine 2020;127:104057.

[11] Andersen RS, Peimankar A, Puthusserypady S. A deep learning approach for real-time detection of atrial fibrillation. Expert Systems with Applications 2019;115:465–473.

[12] Figuera C, Suárez-Gutiérrez V, Hernández-Romero I, Rodrigo M, Liberos A, Atienza F, Guillem MS, Barquero-Pérez Ó, Climent AM, Alonso-Atienza F. Regularization Techniques for ECG Imaging during Atrial Fibrillation: A Computational Study. Frontiers in Physiology oct 2016; 7:466. ISSN 1664-042X.

[13] Cámara-Vázquez MÁ, Oter-Astillero A, Hernández-Romero I, Rodrigo M, Morgado-Reyes E, Guillem MS, Climent AM, Barquero-Pérez Ó. Atrial fibrillation driver localization from body surface potentials using deep learning. In 2020 Computing in Cardiology. IEEE, 2020; 1–4.

[14] García-Molla V, Liberos A, Vidal A, Guillem M, Millet J, González A, et al. Adaptive step {ODE} algorithms for the 3d simulation of electric heart activity with graphics processing units. Computers in Biology and Medicine 2014; 44:15 – 26.

[15] Dössel O, Krueger MW, Weber FM, Wilhelms M, Seemann G. Computational modeling of the human atrial anatomy and electrophysiology. Medical Biological Engineering Computing 2012;50(8):773–799.

[16] Hochreiter S, Schmidhuber J. Long short-term memory. Neural computation 1997;9(8):1735–1780.

[17] Hochreiter S, Schmidhuber J. Long short-term memory. Neural computation 12 1997;9:1735–80.

[18] Vaswani A, Shazeer N, Parmar N, Uszkoreit J, Jones L, Gomez AN, Kaiser Ł, Polosukhin I. Attention is all you need. Advances in neural information processing systems 2017;30.

[19] Goodfellow I, Bengio Y, Courville A. Deep learning. MIT press, 2016.

[20] Stridh M, Bollmann A, Olsson SB, Leif S, et al. Detection and feature extraction of atrial tachyarrhythmias. IEEE Engineering in Medicine and Biology Magazine 2006; 25(6):31–39.

Address for correspondence:

Óscar Barquero-Pérez (oscar.barquero@urjc.es). Dept. III-D217, Camino del Molino, 5. 28943 - Fuenlabrada (Madrid), Spain.